Nitrogen Cycling

Original Research

Open Access

https://doi.org/10.48130/nc-0025-0007

Integrated manure application enhances soil quality and reduces nitrous oxide emissions by deterministically shaping N cycling guilds

Zhujun Wang[1#*], Yue Li[2#], Xinyuan Liu[1] and Xiaotang Ju[1*]

Received: 28 July 2025

Revised: 2 September 2025

Accepted: 19 September 2025

Published online: 17 October 2025

Abstract

A novel application of Infer Community Assembly Mechanisms (iCAMP) reveals how distinct ecological processes governing nitrogen (N) cycling guilds mediate agricultural nitrous oxide (N_2O) emissions. In a long-term field experiment, the guild-specific explanation for how different N fertilizer strategies alter N_2O emissions is provided. No N (N_0), conventional N (N_{con}), optimal N (N_{opt}), and balanced manure with synthetic N (N_{bal} + M) were also compared. The N_{bal} + M treatment significantly enhanced soil quality and maintained high crop yields comparable to the N_{con} treatment. Crucially, N_{bal} + M achieved a lower N_2O emission than N_{con}, a reduction linked to increased abundance of *nosZ* genes. The novel application of iCAMP revealed that this outcome was governed by fundamental shifts in ecological selection. The high N_2O emissions under N_{con} were associated with increased homogeneous selection on N_2O-producers, while the low emissions under N_{bal} + M were driven by decreased homogeneous selection of N_2O-producers and increased homogeneous selection over N_2O-reducers. This study demonstrates that integrated manure application decouples high crop yield from N_2O emissions by predictably shaping the soil microbiome to enhance its N_2O reduction capacity, providing a clear, mechanism-based pathway for developing sustainable agriculture.

Keywords: Nitrous oxide (N_2O), Integrated manure application, Microbial community assembly, *nosZ* gene, Soil quality index

Highlights

- Balanced manure with synthetic N significantly enhances soil quality and crop yield.
- Manure application effectively reduces N_2O emissions compared to conventional fertilization, by stimulating high potential N_2O-reduction related N cycling gene abundances.
- The key nitrifying and denitrifying communities are structured by homogeneous selection.
- A novel application of iCAMP of N cycling functional guilds to explain the N_2O emission under different fertilizer treatments.

Authors contributed equally: Zhujun Wang and Yue Li

* Correspondence: Zhujun Wang (zhujunwang@hainanu.edu.cn); Xiaotang Ju (juxt@cau.edu.cn)

Full list of author information is available at the end of the article.

Graphical abstract

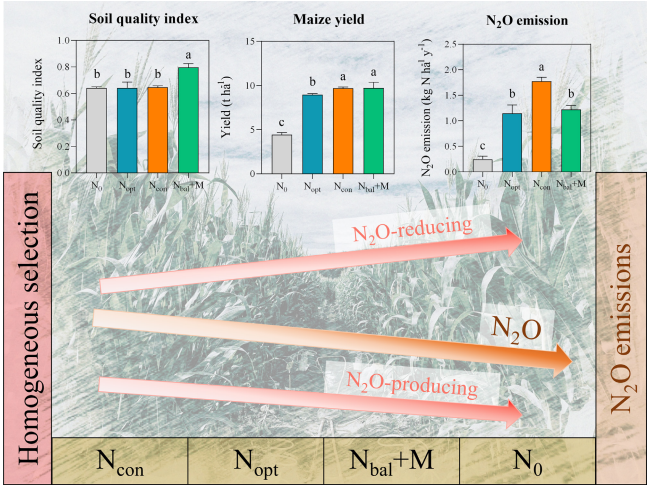

Introduction

The escalating global demand for food has intensified agricultural production, making the application of nitrogen (N) fertilizers a cornerstone of modern agriculture[1]. While essential for achieving high crop yields and ensuring food security, the extensive use of synthetic N fertilizers has created significant environmental challenges[2]. A significant portion of applied N is lost to the environment, contributing to water pollution and the emission of nitrous oxide (N_2O), a potent greenhouse gas with a global warming potential approximately 300 times that of CO_2[3]. Agricultural soils are the largest anthropogenic source of N_2O, placing the management of soil N cycling at the critical relation of food production and climate change mitigation[1].

Soil N_2O emissions are determined by the delicate balance between microbial production and reduction processes, primarily nitrification and denitrification[4]. Nitrification, the oxidation of ammonia to nitrate, can produce N_2O as a byproduct and is carried out by distinct microbial guilds, including archaeal (AOA) and bacterial (AOB) ammonia-oxidizers, as well as comammox bacteria[5]. Denitrification is a stepwise reduction of nitrate to dinitrogen gas (N_2), with N_2O as an intermediate. The final step, the reduction of N_2O to N_2, is catalyzed by the nitrous oxide reductase enzyme, encoded by the *nosZ* gene[6]. Consequently, the N_2O emission potential of a soil is controlled by the relative abundances and diversities of microbial communities harboring genes for N_2O production (e.g., *amoA*, *nirK*, *nirS*) vs N_2O reduction (*nosZ*)[7,8].

The assembly of soil microbial communities is governed by the interplay between deterministic and stochastic processes. Deterministic processes, such as environmental filtering and species competition, involve niche-based selection where the 'fittest' organisms for a given environment are favored, leading to predictable community structures. In contrast, stochastic processes, including dispersal limitation, ecological drift, and random colonization events, result in community patterns that are largely governed by chance[9]. Anthropogenic activities, particularly long-term agricultural fertilization, represent a powerful environmental pressure that can significantly alter the balance between these two forces. It is widely hypothesized that by increasing the availability of limiting nutrients, fertilization imposes strong selective pressures that strengthen the role of determinism, as only a subset of taxa can tolerate or thrive in the altered soil chemistry, such as changes in pH and nutrient concentrations[9]. However, the nature of this shift can depend on the specific fertilization regime; while nutrient enrichment initially increases selection, extreme or unbalanced fertilization might lead to environmental homogenization, which could paradoxically increase the relative importance of stochasticity by weakening niche differentiation among surviving taxa[10,11]. Different agricultural management strategies, such as the use of synthetic versus organic fertilizers, are known to alter these microbial communities. Integrated nutrient management, which combines inorganic fertilizers with organic amendments like manure, has been proposed as a sustainable alternative that can improve soil health and nutrient use efficiency[12,13]. Phylogenetic null model analyses demonstrated that prolonged stover recycling mitigated the processes of dispersal limitation and homogeneous selection in rhizosphere fungal communities, with their formation and maintenance predominantly reliant on stochastic events rather than species' adaptive traits[14]. However, a clear understanding of how these practices specifically influence the key N cycling functional guilds and the ecological processes governing their community assembly is lacking. It is unclear whether the observed changes in N cycling are driven by deterministic selection or by stochastic processes like dispersal limitation, particularly in studies relying primarily on the 16S rDNA or ITS genes[15]. The relative importance of the deterministic and stochastic processes on soil microbial communities varies across environmental gradients, succession stages, and among different assemblages[16,17].

Therefore, understanding how different fertilization strategies modulate the relative influence of determinism and stochasticity is crucial for developing reliable strategies to engineer soil microbiomes for reduced N_2O emissions. This study was designed to investigate the long-term impacts of different fertilizer regimes on soil properties, crop yield, N_2O emissions, and the underlying assembly of N cycling microbial communities. It was hypothesized that: (1) an integrated strategy of balanced manure with synthetic N would maintain high crop yields while mitigating N_2O emissions compared to conventional synthetic N application; (2) this mitigation would be mechanistically driven by a balance of the abundance and diversity of the N_2O-producing and -reducing community; and (3) the assembly of these key N cycling functional guilds would be linked to N_2O emissions. To test these hypotheses, a long-term field experiment consisting of four treatments was set: no fertilizer N applied; optimum rate of chemical N fertilizer; conventional rate of chemical N fertilizer; and balanced manure with synthetic N. This study

employed a multifaceted approach combining measurements of soil physicochemical properties, N-transformation rates, and N_2O fluxes with advanced molecular techniques (qPCR, high-throughput sequencing) and infer community assembly (iCAMP) mechanisms by phylogenetic-bin-based null model analysis to provide a comprehensive, mechanism-based assessment of sustainable nitrogen management in agriculture.

Materials and methods

Site description, experimental design, and sampling

This study was conducted using a long-term field experiment located at the China Agricultural University Research Station in Shangzhuang, Beijing, China (39°48′ N, 116°28′ E, 40 m elevation). The annual mean air temperature and precipitation from 1981 to 2015 were 13.0 °C and 540 mm, respectively. The soil is a typical upland agricultural soil in the North China Plain, characterized by a bulk density of 1.3 g cm^{-3} and a clay loam texture (28.0% clay, 32.0% silt, 40.0% sand, according to the USDA standard). The studied winter wheat–summer maize rotation is the dominant cropping system in this region, in which wheat is sown in early October and harvested in early June of the following year, immediately followed by maize sowing, with harvest occurring in late September.

The long-term field experiment, initiated in October 2006, consisted of four N application rates. The N application treatments were: (1) zero N (N_0), no fertilizer N applied; (2) optimum N (N_{opt}), optimum rates of chemical N fertilizer, determined via the mineral N test method to achieve synchronization of crop N demand with soil N supply; (3) conventional N (N_{con}), conventional rates of chemical N fertilizer according to the local farming practice, with 300.0 and 260.0 kg N ha^{-1} during the wheat and maize seasons, respectively; (iv) balanced manure with synthetic N (N_{bal} + M), in which cattle manure was combined with supplementary chemical fertilizer, calculated to balance crop uptake and soil N surplus. The plot size was 8 × 8 m, and the number of replicates was three. Detailed information, including each N fertilization and irrigation, soil chemical properties for each treatment, and management activities, was described in the previously published papers[18]. Soil samples were collected on 22 July 2022, during the summer maize season, approximately 10 d after N fertilizer application (10 July) at the fourth-leaf growth stages and before the fertilization at the tenth-leaf growth stages (2 August). This sampling timing was deliberately chosen to minimize short-term microbial responses to N application and reflect the long- term effects of different treatments. Furthermore, the summer maize season accounts for up to 84% of annual N_2O emission, as elevated temperatures combined with rainfall enhance microbial activity involved in key nitrogen cycle processes, particularly nitrification and denitrification. Sampling at this period enables assessment of the genetic potential of these active microbial populations. Soil properties in the top 0–20 cm layer from the experimental treatments are shown in Table 1. Soil samples were placed on ice and transported back to the laboratory, where visible grassroots and pebbles were subsequently removed. The soil samples were stored at −80 and 4 °C for DNA extraction and soil geochemical measurements, respectively[19]. The data on cumulative N_2O emissions were cited from Wei et al.[18,20], who measured the N_2O emissions from 2018 to 2019 in the same long-term field experiment. The methods for determining pH, SOC, TN, AK, NH_4^+–N, NO_3^-–N, C/N ratio, PNR, and PDR are provided in Supplementary File 1 (S1.1–S1.3).

Soil quality index and crop yield

Soil quality is determined by various physical, chemical, and biological properties of soil. To assess soil quality consistently and accurately, systematic methods are needed for measuring and interpreting these properties. The soil quality index (SQI) was determined through the following steps[21]: (1) Indicator selection: The evaluation used a dataset including soil pH, SOC, TN, Olsen P, and available K. Principal component analysis (PCA) was applied to select factors from these soil attributes. (2) Indicator scoring and weighting: Each indicator was scored between 0.1 and 1.0 using the standard S equation[22]. The communality of each indicator was extracted by PCA, and weights were calculated as the quotient of each indicator's communality divided by the sum of all communalities. (3) Soil quality index (SQI) calculation: After scoring and weighting, the SQI was calculated using:

$$SQI = \sum_{i=1}^{n} W_i N_i,$$

where, W_i is the assigned weight, N_i is the indicator score, and n is the number of indicators.

At maturity, a 6 m^2 (3 m × 2 m) area of winter wheat and a 10.8 m^2 area (three rows, 6 m long per row) of summer maize were selected to harvest the aboveground crops, which were immediately separated into grains and straw. The samples were then dried separately at 70 °C and weighed to calculate the grain yield.

Sequencing and bioinformatics processing

For bacterial and archaeal 16S rRNA genes, the V4 region was amplified with the primer pair 515F (5'-GTGCCAGCMGCCGCGGTAA-3') and 806R (5'-GGACTACHVGGGTWTCTAAT-3')[23]; the primer pair Arch-amoAF (5'- STAATGGTCTGGCTTAGACG-3') and Arch-amoAR (5'-GCG GCCATCCATCTGTATGT-3') for archaeal *amoA* gene[24]; the primer pair amoA-1F (5'-GGGGTTTCTACTGGTGGT-3') and amoA-2R (5'-CCCC TCKGSAAAGCCTTCTTC-3') for bacterial *amoA* gene[25]; the primer pair comaA-244F (5'-TAYAAYTGGGTSAAYTA-3') and comaA-659R (5'-ARAT CATSGTGCTRTG-3') for comammox *amoA* gene[26]; the primer pair cd3aF (5'- TSAACGTSAAGGARACSGG-3') and R3cd (5'-GASTTCGGRTGS GTCTTGA-3') for *nirS* gene[27]; the primer pair F1aCu (5'-ATCATGGTSCT GCCGCG-3') and R3Cu (5'-GCCTCGATCAGRTTGTGGTT-3') for *nirK* gene[28]; the primer pair nosZ-F (5'-CGYTGTTCMTCGACAGCCAG-3') and nosZ-R (5'-CGSACCTTSTTGCCSTYGCG-3') for *nosZ*I gene[29]; and the primer pair nosZ-II-F (5'-CCTIGGICCIYTKCAYAC-3') and nosZ-II-R (5'-GCIGARCARAAITCBGTRC -3') for *nosZ*II gene[30].

Table 1 Soil properties under different fertilizer treatments while sampling in 2022

Treatment	pH	SOC (g kg^{-1})	TN (g kg^{-1})	C/N	Olsen P (mg kg^{-1})	AK (mg kg^{-1})	NH_4^+-N (mg kg^{-1})	NO_3^--N (mg kg^{-1})	PNR (mg N kg^{-1} h^{-1})	PDR (mg N kg^{-1} h^{-1})
N_0	7.96 ± 0.05 a	6.68 ± 0.19 c	0.72 ± 0.02 c	9.28 ± 0.08 a	28.26 ± 1.36 bc	93.94 ± 4.42 b	0.6 ± 0.06 b	3.03 ± 0.39 b	11.91 ± 1.58 b	0.55 ± 0.07 c
N_{opt}	7.98 ± 0.03 a	7.6 ± 0.6 bc	0.88 ± 0.11 bc	8.74 ± 0.36 a	17.09 ± 1.23 c	116.04 ± 26.8 a	0.91 ± 0.19 a	8.81 ± 1.43 ab	39.58 ± 2.17 ab	0.70 ± 0.03 bc
N_{con}	7.94 ± 0.02 a	7.65 ± 0.47 bc	0.88 ± 0.02 bc	8.66 ± 0.52 a	19.72 ± 2.3 c	92.83 ± 3.32 b	0.94 ± 0.11 a	9.47 ± 1.99 a	41.44 ± 2.12 ab	0.86 ± 0.04 b
N_{bal} + M	7.97 ± 0.01 a	10.33 ± 0.28 a	1.2 ± 0.05 a	8.62 ± 0.34 a	47.9 ± 1.74 a	113.83 ± 5.85 ab	0.85 ± 0.05 ab	8.75 ± 3.57 ab	47.25 ± 1.92 a	1.15 ± 0.06 a

SOC, soil organic carbon; TN, total nitrogen content; AK, available K; NH_4^+–N, ammonium content; NO_3^-–N, nitrate content; PNR, potential nitrification rate; PDR, potential denitrification rate. Different letters indicate the significance among treatments at $p < 0.05$ level by one-way ANOVA. Error bars represent standard deviation ($n = 3$).

The details of qPCR, PCR amplification, amplicon purification, library preparation, Illumina NanoSeq sequencing, and sequence processing were described previously[31,32], and conducted by MAGIGENE company. Amplification conditions for qPCR were as follows: 95 °C for 3 min, 40 cycles of 10 s at 95 °C, 30 s at 52–65 °C, 30 s at 72 °C,and a final extension at 72 °C for 5 min, then held at 16 °C. qPCR amplification efficiencies of these eight genes were between 92% and 105%, and details of Melting Curves are shown in Supplementary File 1 (S1.4). Sequence processing was conducted on an in-house pipeline (https://dmap.denglab.org.cn) integrated with the necessary bioinformatics tools[31–33]. Unoise3[34] was used to remove chimeras and classify the sequences into Amplicon Sequence Variants (ASVs). FrameBot[35] was applied to check and correct the represented nucleotide sequences of ASVs from sequencing samples against the NcycFunGen database (https://ncycfungen.denglab.org.cn)[36] with protein sequences at a high level. The sequencing data are available in the National Microbiology Data Center (https://nmdc.cn/resource/genomics/project) with project number NMDC10019933.

Biodiversity and statistical analysis

Non-metric multidimensional scaling (NMDS) was used to show the differences among the four microbial communities, and the significance of the four fertilizer treatments' contributions to microbial community structure was analyzed by permutational multivariate analysis of variance (PERMANOVA). Further, the relationship between biodiversity and environmental variables was evaluated using the Mantel test. In addition, one-way ANOVA was used to test the differences among multiple groups. All biodiversity and statistical analyses were conducted with an online in-house pipeline (https://dmap.denglab.org.cn)[32,33].

To quantify the underlying mechanisms of microbial community assembly, the study utilised a newly developed method called infer community assembly mechanisms by phylogenetic-bin-based null model analysis (iCAMP)[15]. iCAMP assigns the microbial ASVs into phylogenetic tree-based groups and then quantifies the contribution of each ecological process to microbial community assembly, including homogeneous selection, heterogeneous selection, dispersal limitation, homogenizing dispersal, and undominated processes (drift and others). Null model analysis of the phylogenetic diversity was performed using the beta Net Relatedness Index (βNRI), and taxonomic β-diversities were assessed with the modified Raup–Crick metric (RC). Afterwards, the proportion of each ecological process between different samples was compared based on the bootstrapped methods (n = 1,000). The analyses were conducted with the online pipeline (http://ieg3.rccc.ou.edu:8080)[15], and the other parameters were set to pipeline defaults.

Results

Environmental factors under different fertilizer treatments

Different long-term fertilizer treatments affected key soil properties. There were no significant differences ($p > 0.05$; Table 1) in pH or soil C/N ratio observed among the four fertilizer treatments. In contrast, the N_{bal} + M treatment resulted in the highest concentrations of total N content (TN), soil organic carbon content (SOC), and Olsen P ($p < 0.05$; Table 1). For available K, the N_{opt} treatment recorded the highest value. All fertilizer applications (N_{opt}, N_{con}, N_{bal} + M) significantly increased soil ammonium (NH_4^+–N) and nitrate content (NO_3^-–N) compared to the N_0 control ($p < 0.05$; Table 1). Potential nitrification (PNR) and denitrification rates (PDR) were significantly enhanced by fertilizer application ($p < 0.05$; Table 1). The soil quality index (SQI) was significantly enhanced by N_{bal} + M ($p < 0.05$; Fig. 1a). Crop yield was substantially improved by all fertilization strategies compared to N_0, with the highest yield recorded in the N_{con} and N_{bal}+M ($p < 0.05$; Fig. 1b). Nitrous oxide (N_2O) emissions were significantly influenced by fertilizer application ($p < 0.05$; Fig. 1c). The lowest emission was recorded in the N_0 control, and the highest was in N_{con}.

In summary, N_{bal} + M was the most effective strategy for improving soil quality, significantly increasing SOC, TN, Olsen P, PNR, PDR, SQI, and crop yield, with lower N_2O emissions.

N cycling functional communities under different fertilizer treatments

To investigate the microbial mechanisms underlying the observed changes in nitrogen transformations, the abundances of key functional genes involved in the N cycling, as well as the total bacterial abundance, were quantified via qPCR (Fig. 2). There were no significant differences among the four treatments in 16S rDNA (Fig. 2a), archaeal *amoA* (Fig. 2b), comammox *amoA* (Fig. 2d), *nirK* (Fig. 2e), and *nirS* (Fig. 2f) gene abundance ($p > 0.05$).

N_{con} significantly increased bacterial *amoA* gene abundance compared to the other three treatments ($p < 0.05$; Fig. 2c). However, the abundance of *nosZ* genes, responsible for the final step of denitrification (N_2O reduction to N_2), was significantly influenced by the fertilizer regimes. N_{con} and N_{bal} + M showed the highest *nosZ*I gene abundances ($p < 0.05$; Fig. 2g), while all three fertilizer treatments significantly increased the *nosZ*II gene abundances, with N_{bal} + M being the highest ($p < 0.05$; Fig. 2h).

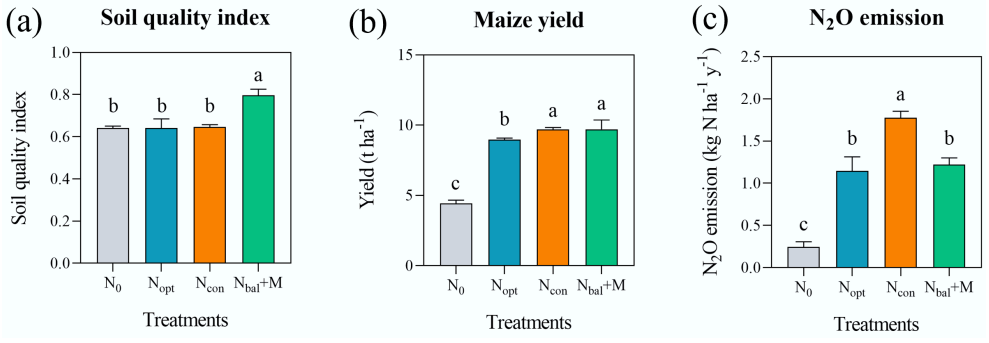

Fig. 1 (**a**) Soil quality index, (**b**) annual maize yield in 2022, and (**c**) average annual N_2O emission from 2018 to 2019 under different fertilizer treatments. N_0: no N, N_{con}: conventional N, N_{opt}: optimal N, N_{bal} + M: balanced manure with synthetic N. Different letters indicate the significance among treatments at $p < 0.05$ level by one-way ANOVA. Error bars represent standard deviation ($n = 3$).

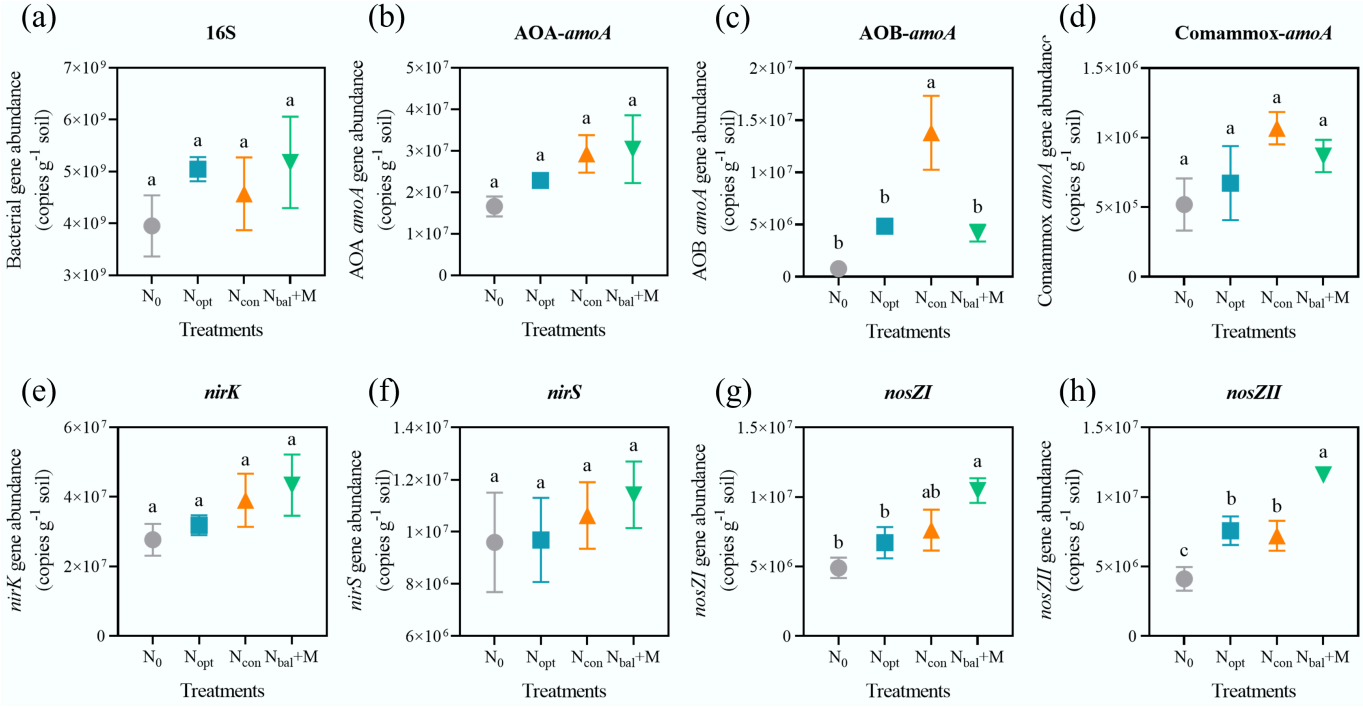

Fig. 2 Nitrogen cycling gene abundances under different fertilizer treatments. (**a**) 16S rDNA. (**b**) Archaeal *amoA* gene. (**c**) Bacterial *amoA* gene. (**d**) Comammox *amoA* gene. (**e**) *nirK* gene. (**f**) *nirS* gene. (**g**) *nosZ*I gene. (**h**) *nosZ*II gene. Different letters indicate the significance among treatments at $p < 0.05$ level by one-way ANOVA. Error bars represent standard deviation ($n = 3$).

To assess the impact of different fertilizer treatments on the community structure of key N cycling genes, Non-metric Multi-dimensional Scaling (NMDS) analysis was performed based on Bray-Curtis dissimilarity. The significance of the community shifts was evaluated using a dissimilarity test (PERMANOVA). The overall bacterial community structure ($p = 0.001$; Fig. 3a), bacterial *amoA* ($p = 0.049$; Fig. 3c), comammox ($p = 0.001$; Fig. 3d), *nirK* ($p = 0.011$; Fig. 3f), and *nosZ*II ($p = 0.001$; Fig. 3h) functional community structures were significantly altered by the fertilizer treatments, with the N_0 samples separating from the fertilized treatments. In contrast, there were no significant differences in archaeal *amoA* ($p > 0.05$; Fig. 3b), *nirS* ($p > 0.05$; Fig. 3e), and *nosZ*I ($p > 0.05$; Fig. 3g) functional community structures under different treatments.

A Mantel test was performed to correlate soil properties and N_2O emissions with the community composition of total bacteria and N functional guilds (Table 2). N_2O emission, SOC, TN, Olsen P, PNR, and PDR were the significant variations correlated to N cycling functional community structures ($p < 0.05$; Table 2). In particular, PNR, PDR, and N_2O emissions were significantly correlated to the denitrifying and comammox communities.

Ecological processes of N cycling functional guilds

The iCAMP analysis was used to quantify the relative influence of deterministic and stochastic processes on the assembly of N cycling functional microbial communities. The analysis partitions community turnover into contributions from homogeneous selection, heterogeneous selection, dispersal limitation, homogenizing dispersal, and drift processes (Fig. 4).

For the total bacterial community (Fig. 4a), stochastic processes were the primary driver, accounting for over 50%, while the contribution of homogeneous selection was 39.2%–41.5%. Distinct assembly mechanisms were observed among the different ammonia-oxidizing guilds. The AOA (Fig. 4b) community assembly was dominated by stochastic processes (over 50%), with homogeneous selection accounting for 30.5%–39.9%. In contrast, the assembly of AOB and comammox communities was predominantly governed by deterministic processes. For the AOB community (Fig. 4c), homogeneous selection accounted for 47.8%–81.2% of the explained processes, with dispersal limitation also playing a notable role (1.9%–38.8%). The comammox community was almost entirely structured by homogeneous selection, which contributed a dominant 66.9%–85.5% to its assembly across all treatments (Fig. 4d). The denitrifier communities also displayed varied assembly patterns. The *nirK*-, *nirS*-, and *nosZ*II-harboring communities were primarily shaped by deterministic processes. Homogeneous selection was the leading factor for these three guilds, accounting for 60.8%–76.7% for *nirK* (Fig. 4e), 41.9%–56.4% for *nirS* (Fig. 4f), and 40.9%–59.1% for *nosZ*II (Fig. 4h). However, the assembly of the *nosZ*I-harboring community (Fig. 4g) was driven by stochastic processes accounting for over 50%.

To further elucidate the influence of fertilization on community assembly, the relative contribution of stochastic processes (including dispersal limitation, homogenizing dispersal, and drift processes) and deterministic processes (heterogeneous and homogeneous selection) were quantified and compared across treatments for each microbial community (Fig. 5). Stochastic processes dominated in 16S DNA (Fig. 5a), AOA (Fig. 5b) and *nosZ*I (Fig. 5g) communities, and deterministic processes dominated in AOB (Fig. 5c), comammox (Fig. 5d), *nirK* (Fig. 5e), *nirS* (Fig. 5f) and *nosZ*II (Fig. 5h) communities.

Deterministicity proportion was significantly different between N_{opt} and N_{con} for the total bacterial community ($p < 0.01$; Fig. 5a). Fertilizer application had divergent and significant effects on the

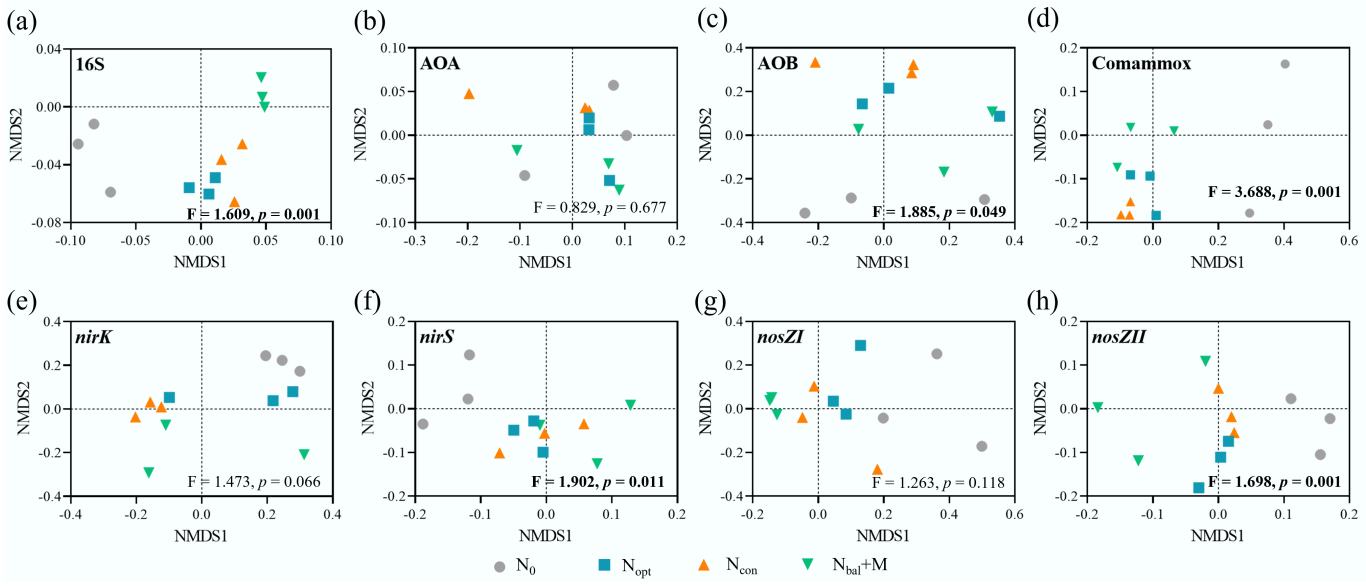

Fig. 3 Effects of different fertilizer treatments on nitrogen functional microbial communities based on NMDS. (**a**) 16S rDNA. (**b**) Archaeal *amoA* gene. (**c**) Bacterial *amoA* gene. (**d**) Comammox *amoA* gene. (**e**) *nirK* gene. (**f**) *nirS* gene. (**g**) *nosZ*I gene. (**h**) *nosZ*II gene. *F*- and *p*-values are based on dissimilarity test.

Table 2 Mantel test of N_2O, soil properties with nitrogen functional microbial communities

	16S		AOA		AOB		Comammox		*nirK*		*nirS*		*nosZ*I		*nosZ*II	
	r	*P*	r	*P*	r	*P*	r	*P*	r	*P*	r	*P*	r	*P*	r	*P*
N_2O (kg N ha^{-1} y^{-1})	**0.456**	**0.007**	−0.004	0.439	**0.343**	**0.017**	**0.733**	**0.001**	0.134	0.194	**0.438**	**0.004**	**0.293**	**0.044**	0.199	0.118
pH	0.053	0.409	−0.122	0.743	−0.078	0.659	0.200	0.126	−0.080	0.606	0.007	0.461	**0.462**	**0.008**	−0.099	0.658
SOC (g kg^{-1})	**0.434**	**0.008**	0.089	0.273	−0.125	0.781	0.201	0.077	**0.280**	**0.045**	0.076	0.313	0.199	0.113	**0.427**	**0.010**
TN (g kg^{-1}	**0.477**	**0.001**	0.014	0.374	−0.135	0.813	0.266	0.053	**0.379**	**0.012**	0.009	0.462	0.154	0.161	**0.411**	**0.006**
C/ N ratio	−0.046	0.570	−0.248	0.992	−0.188	0.908	−0.003	0.457	−0.035	0.529	−0.193	0.880	−0.050	0.561	−0.107	0.710
Olsen P (mg kg^{-1})	**0.336**	**0.036**	0.109	0.223	−0.011	0.407	0.098	0.202	**0.288**	**0.049**	−0.023	0.565	−0.002	0.503	**0.480**	**0.007**
AK (mg kg^{-1})	0.017	0.530	−0.236	0.905	-0.314	0.999	−0.292	0.963	-0.187	0.787	-0.317	0.933	−0.321	0.975	−0.294	0.841
NH_4^+–N (mg kg^{-1})	0.100	0.253	−0.239	0.972	−0.067	0.636	0.113	0.216	−0.094	0.698	0.044	0.365	−0.054	0.582	−0.260	0.945
NO_3^-–N (mg kg^{-1})	0.183	0.141	−0.031	0.516	0.000	0.433	**0.312**	**0.047**	−0.008	0.506	0.223	0.101	0.021	0.408	−0.008	0.486
PNR (mg N kg^{-1} h^{-1})	**0.602**	**0.004**	0.060	0.303	0.129	0.228	**0.795**	**0.003**	**0.318**	**0.042**	**0.459**	**0.005**	**0.471**	**0.008**	**0.320**	**0.045**
PDR (mg N kg^{-1} h^{-1})	**0.626**	**0.001**	0.053	0.339	0.093	0.253	**0.492**	**0.006**	**0.465**	**0.008**	0.252	0.061	0.191	0.147	**0.564**	**0.002**

SOC, soil organic carbon; TN, total nitrogen content; AK, available K; NH_4^+–N, ammonium content; NO^-–N, nitrate content; PNR, potential nitrification rate; PDR, potential denitrification rate. *p*-values shown in bold are significant at the 0.05 level.

assembly processes of different ammonia-oxidizing guilds. For the deterministicity of the AOA community, the value in N_{opt} was significantly higher than in the other three treatments ($p < 0.01$; Fig. 5b). Conversely, for the AOB community (Fig. 5c), all fertilizer treatments significantly decreased the deterministicity proportion compared to the N_0 control ($p < 0.01$). N_{con} exhibited the lowest deterministicity ($p < 0.01$). For the comammox community (Fig. 5d), all fertilizer treatments (N_{opt}, N_{con}, and N_{bal} + M) significantly increased the contribution of deterministicity compared to N_0 ($p < 0.01$).

The assembly of denitrifier communities was also variably affected. For the *nirK*-harboring community, the N_{bal} + M had a significantly lower deterministic proportion than the N_{opt} and N_{con} ($p < 0.01$; Fig. 5e). For the *nosZ*I community, N_{bal} + M significantly increased stochasticity compared to N_0 and N_{con} ($p < 0.01$; Fig. 5g). For *nosZ*II community, N_{con} had a significantly higher determinsticity than N_0 ($p < 0.01$; Fig. 5h). There was no significant difference in the determinsticity proportion observed across treatments for the *nirS*-harboring community.

Discussion

The results revealed the distinct N cycling microbial mechanisms and ecological assembly processes that affected N transformations under different fertilizer regimes. The findings underscore that while conventional synthetic fertilizer application can sustain high yields, it does so at the cost of significant N_2O emissions, driven by specific changes in the nitrifier community. In contrast, the manure-amended system achieves comparable productivity while actively mitigating these emissions by selectively enhancing the soil N_2O reduction capacity.

Integrated nutrient management as a foundation for soil quality and yield productivity

The superiority of balanced manure with synthetic N (N_{bal} + M) treatment is reflected in its benefits for soil quality. The significant increases in SOC, TN, and Olsen P (Table 1) confirm the well-established role of organic amendments in improving long-term soil quality[12]. Unlike synthetic fertilizers that supply specific nutrients, manure provides a complex matrix of carbon compounds and a slow-release source of a

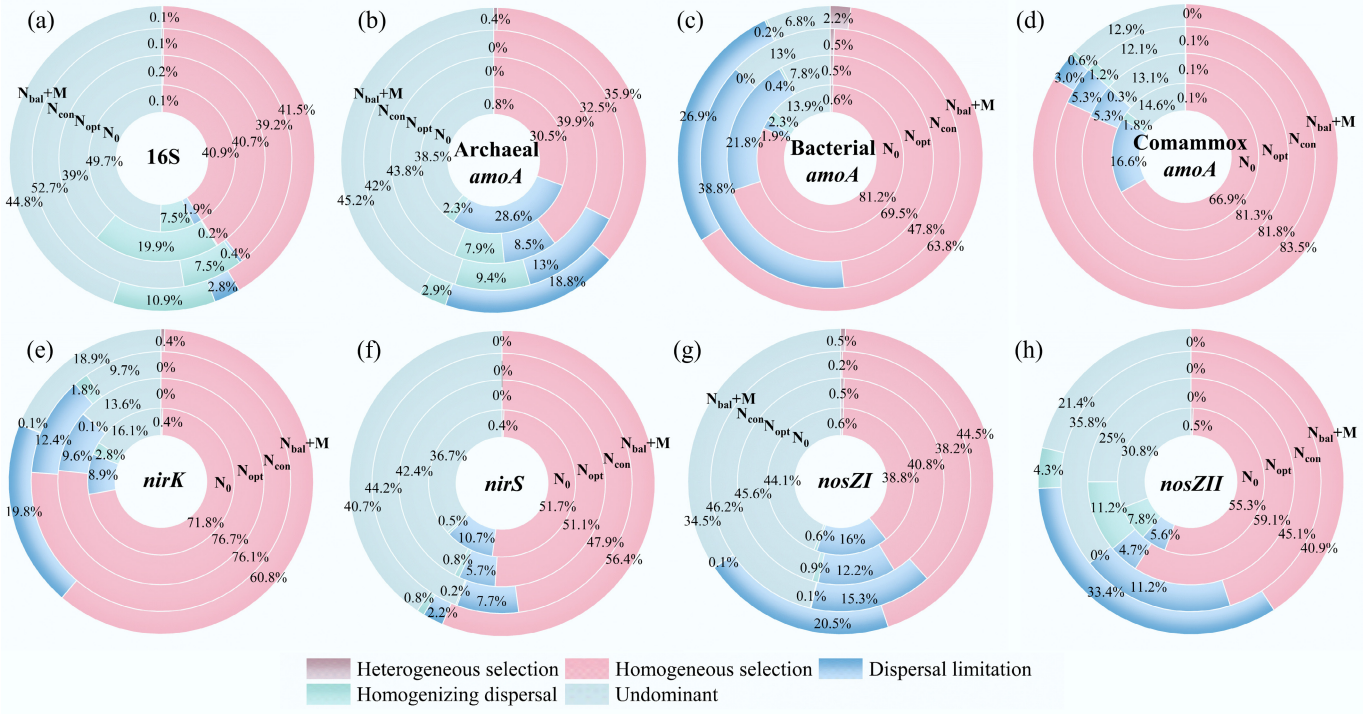

Fig. 4 Proportion of ecological processes for nitrogen functional microbial communities based on bootstrapping results (n = 1,000) from iCAMP. (**a**) 16S rDNA. (**b**) Archaeal *amoA* gene. (**c**) Bacterial *amoA* gene. (**d**) Comammox *amoA* gene. (**e**) *nirK* gene. (**f**) *nirS* gene. (**g**) *nosZ*I gene. (**h**) *nosZ*II gene. Undominant: drift and others.

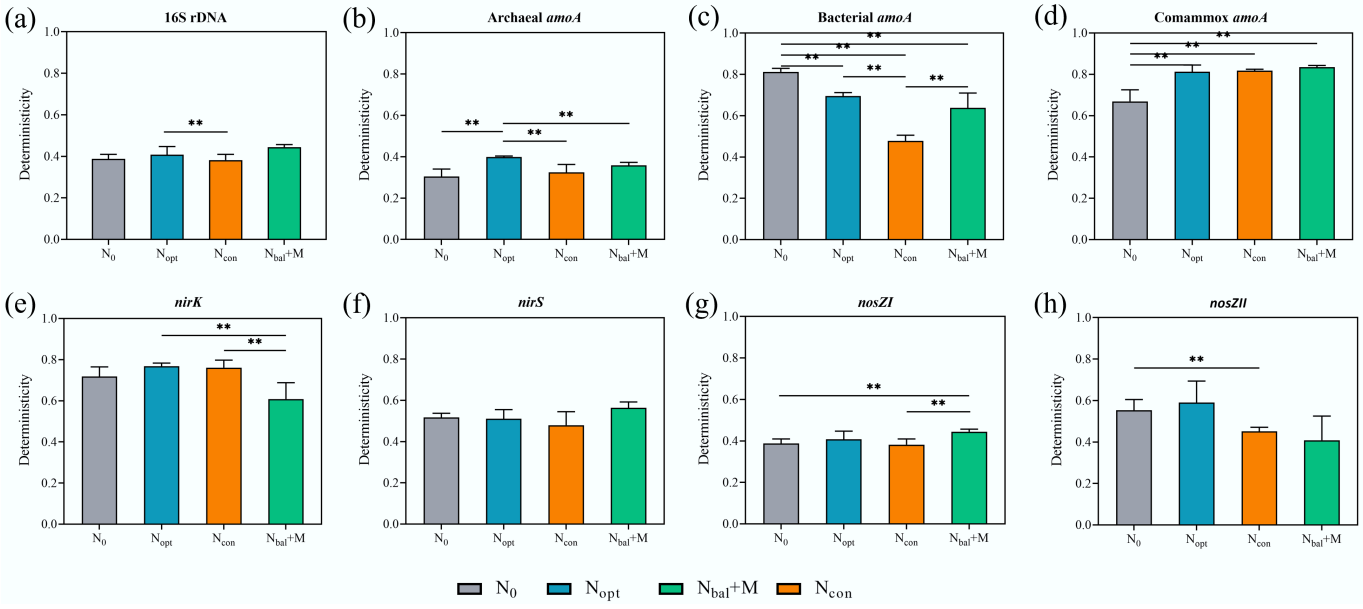

Fig. 5 Deterministicity (presented by homogeneous selection) portion comparison among different fertilizer treatments for nitrogen functional microbial communities based on iCAMP. (**a**) 16S rDNA. (**b**) Archaeal *amoA* gene. (**c**) Bacterial *amoA* gene. (**d**) Comammox *amoA* gene. (**e**) *nirK* gene. (**f**) *nirS* gene. (**g**) *nosZ*I gene. (**h**) *nosZ*II gene. ** $p < 0.01$, * $p < 0.05$. All comparisons show significant differences based on bootstrapping test (n = 1,000).

wide array of nutrients. The resulting elevation of the soil quality index under N_{bal} + M (Fig. 1a) reflects this improvement. The enhanced soil quality translated into crop yields that were statistically similar to those under the highest-input synthetic fertilizer treatments N_{con} and optimate fertilizer input N_{opt} (Fig. 1b). These results suggest that a portion of synthetic fertilizer can be substituted with organic amendments without compromising yield, at least in the context of this study system. The N_{bal} + M strategy thus represents a clear pathway toward sustainable intensification, in which productivity is maintained or enhanced while simultaneously enhancing soil quality.

Decoupling N cycling from N_2O emissions

While all fertilizer treatments stimulated both potential nitrification rate (PNR) and potential denitrification rate (PDR), their ultimate impact on N_2O flux varied, pointing to a critical shift in the balance between N_2O-producing and N_2O-reducing pathways. The high N_2O flux observed

under N_{con} (Fig. 1c) is linked to AOB, whose abundance was highest in this treatment (Fig. 2c). Furthermore, the Mantel test revealed that PNR, PDR, and N_2O emissions were significantly related to the comammox community structure ($p < 0.05$; Table 2). The unresponsiveness of the AOA to fertilization (Figs 2b and 3b), contrasted with the significantly varied AOB and comammox community structures among different treatments ($p < 0.05$; Fig. 3c, d), reinforces the niche differentiation among AOA, AOB, and comammox in dominating the high N nitrification process and its associated emissions[37].

Despite exhibiting the highest PDR, N_{bal} + M had significantly lower N_2O emissions than Ncon (Fig. 1c). N_{bal} + M had significant increase in the abundance of nitrous oxide reductase (*nosZ*) genes (Fig. 2g, h). Furthermore, the Mantel test revealed that PNR and N_2O emission were significantly related to the *nosZ*-harboring community structure, while PDR was related to the *nosZ*II-harboring community ($p < 0.05$; Table 2). The *nosZ*-harboring community, known for its vast phylogenetic diversity and ecological versatility[6], was clearly stimulated by the manure application (Figs 2g, h, and 3g). The carbon and diverse nutrients in manure likely provided the necessary electron donors and cofactors to support a large and active population of these N_2O-reducing heterotrophs[38]. This transforms the soil from a net source to a more efficient sink for N_2O. Validated by the concept that managing agricultural systems to increase the *nosZ* / (*nirS* + *nirK*) gene ratio is a potent strategy for climate change mitigation[39], and the *nosZ*II guild was identified in particular as the key biological lever for achieving this outcome in this study.

Long-term monitoring at our field site demonstrates consistent interannual patterns in N_2O flux responses to different treatments, despite climate variability[18,40,41]. Furthermore, the N_2O emission 'hot moments' are predominantly concentrated on the summer maize season, and the various treatment effects consistently manifested during this period across multiple years. This temporal stability suggests that the underlying microbial mechanisms governing N_2O emissions remain relatively constant at this long-term experimental site. Consequently, by correlating 2022 soil data (reflecting long-term treatment effects on soil properties and microbial communities) with previous annual N_2O emissions, the potential regulatory mechanisms of N-cycling microbes and N_2O production could be explored. Although limited by single-time-point sampling, this approach effectively captures representative microbial drivers.

Deterministic assembly dominates N cycling function guilds

This study provides how deterministic ecological processes govern the assembly of N cycling functionally microbial guilds. While stochastic processes played a significant role in structuring the total bacterial community, the assembly of the most important players in nitrification (AOB, comammox) and denitrification (*nirK*, *nosZ*II) was dominated by homogeneous selection (Fig. 4). This implies that their community structure, and thus their functional capacity, is not a random outcome but a predictable response to the environmental filters imposed by management, varied with the total bacterial community[7]. The assembly of AOA was dominated by stochastic processes, whereas that of AOB was governed by deterministic selection. AOB are classic copiotrophs, adapted to thrive in high-nutrient environments. Fertilization is a powerful and direct environmental filter that deterministically selects for specific, fast-growing AOB taxa[42], a conclusion supported by the significant increase in AOB abundance under the N_{con} treatment (Fig. 2). In contrast, AOA are oligotrophs with a high-affinity ammonia oxidation system, which makes them superior competitors in low-N conditions. In the absence of a strong filter favoring their growth, the AOA community composition is more susceptible to stochastic processes like ecological drift and dispersal from the regional species pool[43].

Furthermore, N_2O emission was significantly related to comammox, *nirK*, *nosZ*I, and *nosZ*II community structure (Table 2). N_{con} treatment, which had the highest N_2O emission, exhibited lower homogeneous selection in *nosZ*I and *nosZ*II communities, and higher homogeneous selection in comammox and *nirK* communities, along with significantly different homogeneous selection portions compared to N_{bal} + M in *nirK* and *nosZ*I communities (Fig. 5). These findings indicate that the microbial assembly mechanisms underlying N_2O emission involve increased homogeneous selection in N_2O-producing communities and decreased homogeneous selection in N_2O-reducing communities.

Moreover, the *nosZ*I community was primarily shaped by stochastic processes, while the *nosZ*II community was structured by deterministic selection. This can be attributed to their distinct phylogenetic diversity and ecological niches[6]. *nosZ*II is known to be more phylogenetically diverse and ecologically versatile, found in a wider range of microorganisms (including non-denitrifiers) and habitats[44]. Crucially, many *nosZ*II-containing organisms can reduce N_2O under microaerobic conditions, which makes them highly adaptable to the fluctuating oxygen levels typical of agricultural topsoil. While the *nosZ*I guild, often associated with 'canonical' denitrifiers in more strictly anaerobic niches, may find its activity limited to transient, spatially-patchy anaerobic microsites within the soil matrix[38]. Their assembly would therefore be less influenced by the overarching management strategy and more by unpredictable, localized conditions, appearing as a stochastic process at the scale of our investigation. This highlights that even within the same functional step, different clades can be governed by different ecological rules.

Limitations and future directions

Despite the mechanistic insights provided by this study, several limitations should be acknowledged to contextualize the findings and guide future work. First, the experiment was conducted at a single site within the North China Plain, characterized by a specific clay loam soil and an intensive winter wheat–maize cropping system. The magnitude of treatment effects on microbial community assembly and N_2O fluxes is likely dependent on local soil properties and climate. Therefore, validating these findings across a broader range of agroecological zones is a critical next step to ascertain the universality of the observed mechanisms.

Second, although this study effectively demonstrates the potential of integrated manure management, the scalability of this practice faces practical and economic hurdles. The composition of manure varies significantly with animal source and storage method, which could alter its effect on the soil microbiome. Furthermore, widespread adoption depends on factors such as local manure availability, transportation costs, and the economic viability for farmers compared to synthetic fertilizers. Future research should integrate socioeconomic analysis and explore different types of organic amendments to develop strategies that are both ecologically sound and practically scalable. Finally, although the single-time-point microbial sampling was strategically timed to reflect long-term effects, it does not capture the intra-annual dynamics of the N-cycling communities. Future studies incorporating high-frequency temporal sampling would provide a more complete picture of how microbial assembly processes shift in response to fertilization, irrigation, and crop growth stages.

In conclusion, this investigation demonstrates that sustainable N management hinges on steering microbial ecological processes. A novel application of iCAMP to N-cycling functional guilds explains

how N_2O emissions are regulated by the balance of deterministic and stochastic forces shaping community assembly. Key guilds involved in nitrification (AOB, comammox) and denitrification (*nirK*, *nosZ*II) were primarily structured by homogeneous selection, implying that their composition is a predictable response to environmental filters imposed by fertilizer management. The high N_2O emission under conventional fertilization corresponds to stronger deterministic control over N_2O-producing communities, making high emissions a predictable outcome. In contrast, integrated manure application mitigates N_2O by shifting this balance: it weakens homogeneous selection on N_2O-producers while strengthening it for N_2O-reducers. This approach moves beyond simply supplying nutrients to actively curating a soil microbiome that is more efficient at N_2O reduction. This study provides a mechanistic roadmap for this ecological engineering, demonstrating that by managing the underlying assembly processes of the N-cycle, the critical goal of high-yield agriculture can be achieved with a smaller environmental footprint.

Supplementary information

It accompanies this paper at: https://doi.org/10.48130/nc-0025-0007.

Author contributions

The authors confirm their contributions to the paper as follows: study conception and design, draft manuscript preparation: all authors; original research plan, all site experiments setup: Ju X; sampling implementation, the soil experiments, sequencing, and data analysis: Wang Z, Li Y. All authors reviewed the results and approved the final version of the manuscript.

Data availability

The sequencing data are available in National Microbiology Data Center (https://nmdc.cn/resource/genomics/project) with project number NMDC10019933.

Funding

This work was supported by the National Natural Science Foundation of China (Grant No. U24A20625).

Declarations

Competing interests

The authors declare that they have no conflict of interest.

Author details

[1]School of Tropical Agriculture and Forestry, Hainan University, Haikou 570228, China; [2]Institute of Applied Ecology, Chinese Academy of Sciences, Shenyang 110016, China

References

[1] Ju X, Xing G, Chen X, Zhang S, Zhang L, et al. 2009. Reducing environmental risk by improving N management in intensive Chinese agricultural systems. *Proceedings of the National Academy of Sciences of the United States of America* 106:3041–3046

[2] Foley JA, Ramankutty N, Brauman KA, Cassidy ES, Gerber JS, et al. 2011. Solutions for a cultivated planet. *Nature* 478:337–342

[3] Calvin K, Dasgupta D, Krinner G, Mukherji A, Thorne PW, et al. 2023. Climate change 2023. *R6 Synthesis report*. Contribution of working groups i, ii and iii to the sixth assessment report of the intergovernmental panel on climate change. Intergovernmental panel on climate change, Geneva, 2023. Switzerland. pp. 1–34 doi: 10.59327/IPCC/AR6-9789291691647

[4] Stein LY, Klotz MG. 2016. The nitrogen cycle. *Current Biology* 26:R94–R98

[5] Daims H, Lebedeva EV, Pjevac P, Han P, Herbold C, et al. 2015. Complete nitrification by Nitrospira bacteria. *Nature* 528:504–509

[6] Hallin S, Philippot L, Löffler FE, Sanford RA, Jones CM. 2018. Genomics and ecology of novel N_2O-reducing microorganisms. *Trends in Microbiology* 26:43–55

[7] Xu S, Yu Y, Fan H, Bilyera N, Meng X, et al. 2024. Microbial communities overwhelm environmental controls in explaining nitrous oxide emission in acidic soils. *Soil Biology and Biochemistry* 194:109453

[8] Soler-Jofra A, Pérez J, van Loosdrecht MCM. 2021. Hydroxylamine and the nitrogen cycle: A review. *Water Research* 190:116723

[9] Zhou J, Deng Y, Zhang P, Xue K, Liang Y, et al. 2014. Stochasticity, succession, and environmental perturbations in a fluidic ecosystem. *Proceedings of the National Academy of Sciences of the United States of America* 111:E836–E845

[10] Dini-Andreote F, Stegen JC, van Elsas JD, Salles JF. 2015. Disentangling mechanisms that mediate the balance between stochastic and deterministic processes in microbial succession. *Proceedings of the National Academy of Sciences of the United States of America* 112:E1326–E1332

[11] Tripathi BM, Stegen JC, Kim M, Dong K, Adams JM, et al. 2018. Soil pH mediates the balance between stochastic and deterministic assembly of bacteria. *The ISME Journal* 12:1072–1083

[12] Montemurro F, Vitti C, Diacono M, Canali S, Tittarelli F, Ferri DJFEB. 2010. A three-year field anaerobic digestates application: effects on fodder crops performance and soil properties. *Fresenius Environmental Bulletin* 19:2087–2093

[13] Gu B, Ju X, Chang J, Ge Y, Vitousek PM. 2015. Integrated reactive nitrogen budgets and future trends in China. *Proceedings of the National Academy of Sciences of the United States of America* 112:8792–8797

[14] Liu Q, Kong X, Wu W, Jiao Y, Yue S, et al. 2025. Rain-fed spring maize exhibits growth stability through rhizosphere microbial responses to stover return and organic fertilizer application. *Plant and Soil*

[15] Ning D, Yuan M, Wu L, Zhang Y, Guo X, et al. 2020. A quantitative framework reveals ecological drivers of grassland microbial community assembly in response to warming. *Nature Communications* 11:4717

[16] Liu N, Hu H, Ma W, Deng Y, Wang Q, et al. 2021. Relative importance of deterministic and stochastic processes on soil microbial community assembly in temperate grasslands. *Microorganisms* 9:1929

[17] Wang Z, Feng K, Lu G, Yu H, Wang S, et al. 2022. Homogeneous selection and dispersal limitation dominate the effect of soil strata under warming condition. *Frontiers in Microbiology* 13:801083

[18] Wei H, Song X, Liu Y, Wang R, Zheng X, et al. 2023. In situ ^{15}N–N_2O site preference and O_2 concentration dynamics disclose the complexity of N_2O production processes in agricultural soil. *Global Change Biology* 29:4910–4923

[19] Wang Z, Lu G, Yuan M, Yu H, Wang S, et al. 2019. Elevated temperature overrides the effects of N amendment in Tibetan grassland on soil microbiome. *Soil Biology and Biochemistry* 136:107532

[20] Wei H, Li Y, Zhu K, Ju X, Wu D. 2024. The divergent role of straw return in soil O_2 dynamics elucidates its confounding effect on soil N_2O emission. *Soil Biology and Biochemistry* 199:109620

[21] Shukla MK, Lal R, Ebinger M. 2006. Determining soil quality indicators by factor analysis. *Soil and Tillage Research* 87:194–204

[22] Qi Y, Darilek JL, Huang B, Zhao Y, Sun W, et al. 2009. Evaluating soil quality indices in an agricultural region of Jiangsu Province, China. *Geoderma* 149:325–334

[23] Caporaso JG, Lauber CL, Walters WA, Berg-Lyons D, Lozupone CA, et al. 2011. Global patterns of 16S rRNA diversity at a depth of millions of sequences per sample. *Proceedings of the National Academy of Sciences of the United States of America* 108:4516–4522

[24] Francis CA, Roberts KJ, Beman JM, Santoro AE, Oakley BB. 2005. Ubiquity and diversity of ammonia-oxidizing archaea in water columns and

sediments of the ocean. *Proceedings of the National Academy of Sciences of the United States of America* 102:14683–14688
[25] Rotthauwe JH, Witzel KP, Liesack W. 1997. The ammonia monooxygenase structural gene amoA as a functional marker: molecular fine-scale analysis of natural ammonia-oxidizing populations. *Applied and Environmental Microbiology* 63:4704–4712
[26] Pjevac P, Schauberger C, Poghosyan L, Herbold CW, van Kessel MAHJ, et al. 2017. *AmoA*-targeted polymerase chain reaction primers for the specific detection and quantification of comammox *Nitrospira* in the environment. *Frontiers in Microbiology* 8:1508
[27] Throbäck IN, Enwall K, Jarvis Å, Hallin S. 2004. Reassessing PCR primers targeting nirS, nirK and nosZ genes for community surveys of denitrifying bacteria with DGGE. *FEMS Microbiology Ecology* 49:401–17
[28] Hallin S, Lindgren PE. 1999. PCR detection of genes encoding nitrite reductase in denitrifying bacteria. *Applied and Environmental Microbiology* 65:1652–1657
[29] Kloos K, Mergel A, Rösch C, Bothe H. 2001. Denitrification within the genus Azospirillum and other associative bacteria. *Functional Plant Biology* 28:991–998
[30] Jones CM, Graf DRH, Bru D, Philippot L, Hallin S. 2013. The unaccounted yet abundant nitrous oxide-reducing microbial community: a potential nitrous oxide sink. *The ISME Journal* 7:417–426
[31] Wei Z, Liu Y, Feng K, Li S, Wang S, et al. 2018. The divergence between fungal and bacterial communities in seasonal and spatial variations of wastewater treatment plants. *Science of The Total Environment* 628–629:969–978
[32] Feng K, Wang S, He Q, Bonkowski M, Bahram M, et al. 2024. CoBacFM: Core bacteria forecast model for global grassland pH dynamics under future climate warming scenarios. *One Earth* 7:1275–1287
[33] Feng K, Zhang Z, Cai W, Liu W, Xu M, et al. 2017. Biodiversity and species competition regulate the resilience of microbial biofilm community. *Molecular Ecology* 26:6170–6182
[34] Edgar RC. 2016. UNOISE2: improved error-correction for Illumina 16S and ITS amplicon sequencing. *bioRxiv* 081257
[35] Wang Q, Quensen JF, Fish JA, Lee TK, Sun Y, et al. 2013. Ecological patterns of nifH genes in four terrestrial climatic zones explored with targeted metagenomics using FrameBot, a new informatics tool. *MBio* 4:e00592–13
[36] Wang Z, Feng K, Wei Z, Wu Y, Isobe K, et al. 2022. Evaluation and redesign of the primers for detecting nitrogen cycling genes in environments. *Methods in Ecology and Evolution* 13:1976–1989
[37] Li C, Hu HW, Chen QL, Chen D, He JZ. 2020. Niche differentiation of clade A comammox Nitrospira and canonical ammonia oxidizers in selected forest soils. *Soil Biology and Biochemistry* 149:107925
[38] Li Z, Yang Y, Wang X, Qi Y, Yang X. 2025. Linking N_2O emissions and nosZ gene abundance: a meta-analysis of organic carbon amendments in agricultural soils. *Plant and Soil*
[39] Graf DRH, Jones CM, Hallin S. 2014. Intergenomic comparisons highlight modularity of the denitrification pathway and underpin the importance of community structure for N_2O emissions. *PLoS One* 9:e114118
[40] Song X, Ju X, Topp CFE, Rees RM. 2019. Oxygen regulates nitrous oxide production directly in agricultural soils. *Environmental Science & Technology* 53:12539–12547
[41] Huang T, Yang H, Huang C, Ju X. 2017. Effect of fertilizer N rates and straw management on yield-scaled nitrous oxide emissions in a maize-wheat double cropping system. *Field Crops Research* 204:1–11
[42] Mushinski RM, Phillips RP, Payne ZC, Abney RB, Jo I, et al. 2019. Microbial mechanisms and ecosystem flux estimation for aerobic NOy emissions from deciduous forest soils. *Proceedings of the National Academy of Sciences of the United States of America* 116:2138–45
[43] Ayala-Ortiz C, Freire-Zapata V, Tfaily MM. 2025. Stochastic assembly and metabolic network reorganization drive microbial resilience in arid soils. *Communications Earth & Environment* 6:647
[44] Xu X, Liu Y, Singh BP, Yang Q, Zhang Q, et al. 2020. *NosZ* clade II rather than clade I determine in situ N_2O emissions with different fertilizer types under simulated climate change and its legacy. *Soil Biology and Biochemistry* 150:107974